

Strain Dependent Electronic Properties of Hexagonal Monolayer Boron Phosphide with GPAW using GLLB-SC and PBE

Polat NARİN^{1*} 

¹AYBU Central Research Laboratory, Ankara Yıldırım Beyazıt University, Ankara 06050, Türkiye

Article Info

Research article
Received: 13/09/2022
Revision: 26/12/2022
Accepted: 27/12/2022

Keywords

DFT
Hexagonal Boron
Phosphide
2D materials
GLLB-SC
PBE

Makale Bilgisi

Araştırma makalesi
Başvuru: 13/09/2022
Düzeltilme: 26/12/2022
Kabul: 27/12/2022

Anahtar Kelimeler

YFT
Hekzagonal Bor
Fosfat
2B malzemeler
GLLB-SC
PBE

Graphical/Tabular Abstract (Grafik Özet)

In this study, the strain-dependent electronic properties of monolayer h-BP are studied by DFT method using GPAW. Applying strain to h-BP monolayer shows the tunable electronic band gap. / Bu çalışmada, gerginliğe bağlı hekzagonal bor fosfat tek tabakanın elektronik özellikleri GPAW kullanılarak YFT yöntemiyle çalışılmıştır. h-BP'a uygulanan gerginlik ile ayarlanabilir elektronik bant aralığı elde edilmiştir.

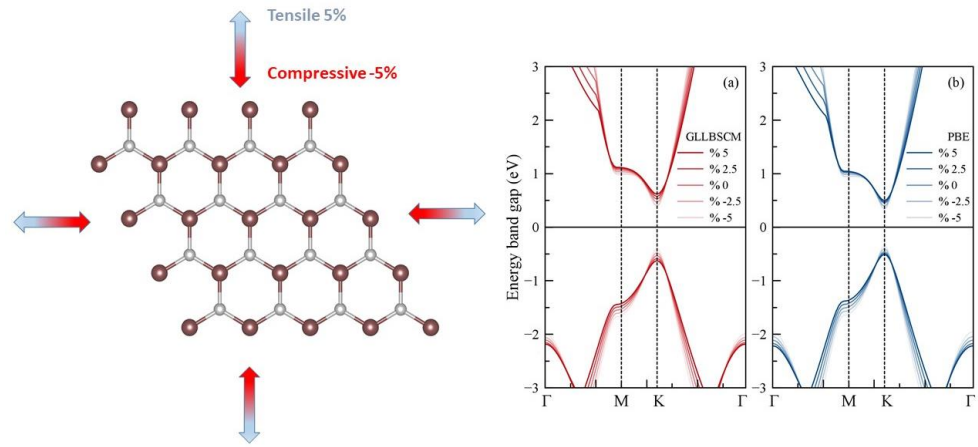


Figure A: Applying strain and electronic band structures of h-BP monolayer / Şekil A: Uygulanan gerginlik ve h-BP tek tabakanın elektronik bant yapıları.

Highlights (Önemli noktalar)

- The strain dependent electronic properties of h-BP monolayer have been investigated. / Gerginlik bağlı h-BP tek tabakanın elektronik özellikleri incelenmiştir.
- GLLB-SC is more accurately calculated the electronic band structure of h-BP monolayer than PBE. / GLLB-SC h-BP tek tabakanın elektronik bant yapısının PBE'den daha doğru hesaplamaktadır.
- h-BP monolayer has been shown a tunable band gap with strain. / h-BP gerginlik ile ayarlanabilir bant aralığı göstermiştir.

Aim (Amaç): In this study, it is aimed to calculate the electronic band structure of h-BP using GPAW. Also it is aimed to calculate the strain-dependent electronic band structure of h-BP monolayer using GLLB-SC and PBE. / Bu çalışmada h-BP tek tabakanın elektronik bant yapısını GPAW kullanılarak hesaplanması amaçlanmıştır. Ayrıca gerginliğe bağlı olarak h-BP tek tabakanın elektronik özellikleri GLLB-SC ve PBE kullanılarak hesaplanması amaçlanmıştır.

Originality (Özgünlük): The strain-dependent electronic properties of h-BP using GPAW have been investigated for the first time. / Gerginliğe bağlı h-BP tek tabakanın elektronik özellikleri GPAW kullanılarak ilk kez incelenmiştir.

Results (Bulgular): The electronic properties of h-BP monolayer have been investigated. The found electronic band gap values have been compared with the literature's results. It is found that GLLB-SC has more accurately calculated the electronic band structure than PBE. / h-BP tek tabakanın elektronik özellikleri incelenmiştir. GLLB-SC, h-BP'in elektronik bant yapısını PBE'den daha doğru hesapladığı bulunmuştur.

Conclusion (Sonuç): This study shows the results of the electronic band structure of h-BP under strain using GPAW. As result of this study, applying strain to h-BP is to change the electronic band structure. / Bu çalışma GPAW kullanılarak gerginlik altında h-BP'in elektronik bant yapısının sonuçlarını göstermektedir. Bu çalışmanın sonucu olarak, h-BP tek tabakaya gerginlik uygulamak elektronik bant yapısını değiştirmektedir.



Strain Dependent Electronic Properties of Hexagonal Monolayer Boron Phosphide with GPAW using GLLB-SC and PBE

Polat NARİN^{1*}

¹AYBU Central Research Laboratory, Ankara Yıldırım Beyazıt University, Ankara 06050, Türkiye

Article Info

Research article
Received: 13/09/2022
Revision: 26/12/2022
Accepted: 27/12/2022

Keywords

DFT
Hexagonal Boron
Phosphide
2D materials
GLLB-SC
PBE

Abstract

Two dimensional materials (2D) like Graphene have a big importance due to their unique electronic properties. In numerical calculations, the electronic properties of 2D materials have been studied using *ab initio* methods. For this reason, in this study, the electronic properties of the hexagonal Boron Phosphide (h-BP) monolayer have been investigated by first-principles calculations. The electronic band structure of the h-BP monolayer has been calculated using GPAW with PBE and GLLB-SC exchange correlations (XCs). In this study, GLLB-SC has been used to investigate the electronic properties of h-BP for the first time. The energy band gaps of the h-BP monolayer are found to be 0.89 eV and 1.05 eV for PBE and GLLB-SC, respectively. It is shown that GLLB-SC in calculations as XC ensures a more accurate energy band gap than the PBE. As well as the electronic calculations of the unstrained h-BP monolayer, the strain calculations are performed between +5 and -5 %. The strain in the h-BP monolayer changed the energy band gap between 0.78 eV and 1.24 eV for GLLB-SC and between 0.66 eV and 1 eV for PBE. In this applied strain range the studied structure shows the direct band gap semiconductor behavior. Furthermore, strain-dependent tunable energy band gap has been obtained as a result of the calculations.

GLLB-SC ve PBE kullanılarak GPAW ile Hekzagonal Tek Tabakalı Bor Fosfatın Gerginliğe Bağlı Elektronik Özellikleri

Makale Bilgisi

Araştırma makalesi
Başvuru: 13/09/2022
Düzeltilme: 26/12/2022
Kabul: 27/12/2022

Anahtar Kelimeler

YFT
Hekzagonal Bor
Fosfat
2B malzemeler
GLLB-SC
PBE

Öz

Grafen benzeri iki boyutlu malzemeler (2B) eşsiz özellikleri sebebiyle büyük bir öneme sahiptir. Hesaplamalı çalışmalarda, 2B malzemelerin elektronik özellikleri *ab initio* metodları kullanılarak hesaplanmıştır. Bu sebeple, bu çalışmada, hekzagonal Bor Fosfat (h-BP) tek tabakanın elektronik özellikleri ilk prensipler ile hesaplanmıştır. H-BP tek tabakanın elektronik özellikleri GPAW ile PBE ve GLLB-SC değiş tokuş korelasyonları kullanılarak hesaplanmıştır. Bu çalışmada, h-BP tek tabakanın elektronik özelliklerini incelemek için ilk kez GLLB-SC kullanılmıştır. H-tek tabaka için yasak bant aralığı değerleri sırasıyla PBE ve GLLB-SC için 0.89 eV ve 1.05 eV olarak hesaplanmıştır. Değiş tokuş korelasyonu olarak GLLB-SC yönteminin, PBE'den daha doğru sonuç verdiği görülmektedir. Gerginlik olmadığı durumda h-BP tek tabakanın elektronik hesaplarının yanı sıra, +5% ve -5% aralığında gerginliğe sahip örgü için elektronik hesaplamalar gerçekleştirilmiştir. H-BP tek tabaka'daki gerginlik GLLB-SC yöntemi ile hesaplandığında yasak bant aralığını 0.78 eV ve 1.24 eV aralığında, PBE yöntemi için ise 0.66 eV ve 1 eV aralığında değiştirmiştir. Uygulanan gerginlik aralığında, h-BP direk geçişli yarıiletken davranışı sergilemiştir. Bunlara ek olarak hesaplamaların sonucunda h-BP'da gerginliğe bağlı olarak ayarlanabilir yasak bant aralığı elde edilmiştir.

1. INTRODUCTION (GİRİŞ)

Two-dimensional (2D) materials have been attracted over the past years. Since 2D materials have been studied electronic-based applications such as field effect transistors, high-frequency electronics, 2D flexible electronic applications etc.[1] Among these applications, some of these are

Li/Na-ion batteries of graphene and sub-10 nm transistors of MoS₂ [2]. These examples give a fingerprint about the importance of 2D because it is required a few layer thicknesses of 2D materials to build nanometer-scale devices. In flexible sensor applications, the flexible and ultrathin piezoelectrics properties of 2D layered materials like MoS₂ are used [3]. Moreover, the lack of

inversion symmetry in InSe, GaS monolayers produces high large in-plane piezoelectric properties [4]. These above unique properties of 2D materials are still being studied. Transition-metal di-chalcogenides (TMDs), buckled and puckered 2D materials such as silicene, germanene, phosphorene, etc. are recent 2D material groups [5-8]. Similar to these materials, III-V group monolayers including hexagonal crystal systems are another planar important 2D materials [9]. Well-known hexagonal boron nitride (h-BN) is one of the III-V monolayers that has a wide band gap energy of ~6 eV. Similar to the hexagonal honeycomb crystal structure of h-BN, hexagonal boron phosphide (h-BP monolayer) has attracted over the last years due to direct semiconductor behavior, energetically stability, small effective mass, and high carrier mobility [10-12].

The energy band gap of the h-BP monolayer is nearly 0.8 eV for PBE in density functional theory (DFT) calculations [13]. Some studies calculated by different exchange-correlation (XC) energy functionals such as hybrid HSE06 and GW a show higher energy band gap than PBE results [14, 15]. In recent years, fast XC functionals such as meta-GGA, modified Becke-Johnson (mBJ), *etc.* are used to reduce the computational expensiveness compared to hybrid HSE06 and GW [16]. Another importance of these types of XC functionals is lower absolute relative errors (15%-40%) than PBE (50%) [17]. However, this absolute relative error is strongly dependent on chosen materials type [18]. As well as HSE06 and GW, GLLB-SC XC functional purposed by Gritsenko, van Leeuwen, van Lenthe, and Baerends (GLLB) and for solids and correlation (SC) called as GLLB-SC are calculated similarly to HSE06's results [19]. Also, GLLB-SC is implemented in GPAW code and used for DFT calculations [20]. GLLB-SC is known to give similar lower absolute relative error just as mBJ and meta-GGA.

The electronic behavior of the h-BP monolayer could be tunable with the external electric field, strain in the lattice, doping, *etc.* [13, 21, 22]. Among these, the strain is usually used to control the bandgap for many 2D materials [23]. In PBE and HSE06 calculations of the h-BP monolayer showed that as long as from compressive (blue shift) to tensile (redshift) strain on the lattice is applied, the electronic band gap is increased [24]. However, these calculations are not yet investigated by GLLB-SC. Therefore, in this study, the strain-dependent calculations between -5% and +5% of h-BP monolayer have been investigated to determine electronic structure with PBE and GLLB-SC.

2. MATERIALS AND METHODS (MATERİYAL VE METOD)

2.1. Computational Details (Hesaplama Detayları)

First principle calculations have been performed using a grid-based projector-augment wave (GPAW) code-[25]. To reduce the complexity in preparing input, *gpaw-tools* written by Lisesivdin *et. al.* are used [26]. The *gpaw-tools* are very useful at each step of the input preparation and result processing. Before the electronic structure calculations of h-BP, some optimizations have been made. For optimizations, the lattice as shown in figure 1 which has illustrated the configuration of the planar h-BP monolayer and also observed unit-cell with a black line has been used. The k-points and cut-off values are used 9x9x1 and 450 eV both PBE and GLLB-SC functionals, respectively. GLLB-SC is not allowed geometry optimization; hence, both XCs have performed optimizations. The lattice optimization calculations were done for both PBE and GLLB-SC XCs.

Figure 2 shows the energy dependence of the lattice parameters of h-BP. The calculated energy-dependent lattice parameters for both are fitted and found to be 3.2074 Å for PBE and 3.2068 Å for GLLB-SC for minimum total energy values. Along the z-axis, c the parameter is kept as 20 Å to avoid interaction between planes. After optimizations of k-point, cut-off, and the lattice parameters of h-BP, the electronic band structure, density of states (DOS), and projected DOS (PDOS) of the h-BP monolayer have been calculated unstrained by both PBE and GLLB-SC. To investigate the effect of strain on the electronic results of h-BP, the strain values between -5% and +5% are applied with changing lattice parameters eq.(1). The electronic band structures and the energy band gaps are calculated depending on the strain in the lattice. Using these unstrained lattice parameters of the h-BP, the strained lattice parameters are calculated in the following equation;

$$\varepsilon = (a - a_0)/a_0 \quad (1)$$

Where ε is the strain, a_0 and a are unstrained and strained lattice parameters of the h-BP, respectively. Also, due to $a=b$ of h-BP, the strain equation is only given for a parameter. However, in calculations, the biaxial strain is applied to both lattice parameters of h-BP.

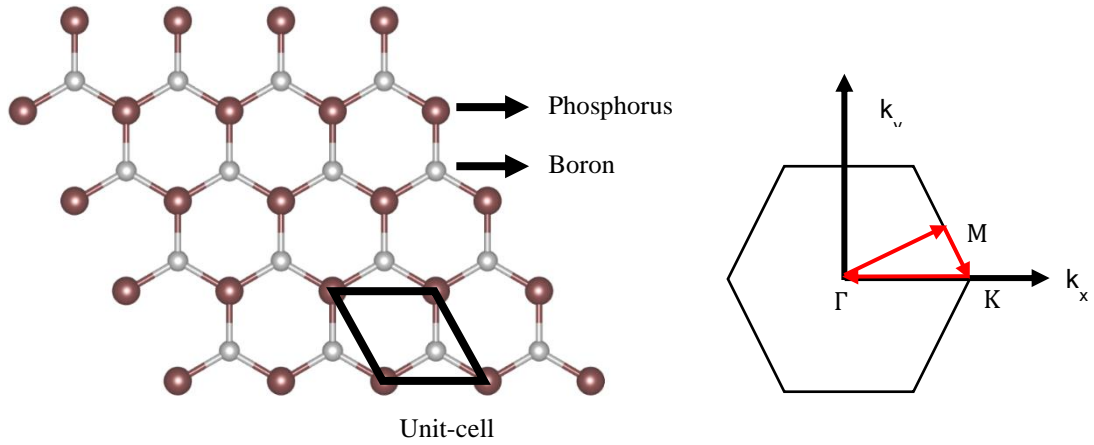


Figure 1. In left side the atomic configuration of h-BP monolayer and in right side schematic Brillouin zone for h-BP which uses in planar hexagonal lattice the used brillioun path also shown with red arrows Γ -M-K- Γ . The used unit cell of h-BP is shown as black line. In atomic configuration of h-BP brown and gray spheres represent Phosphorus and Boron atoms, respectively (Sol tarafta h-BP'in atomik konfigürasyonu, sağ tarafta düzlem hekzagonal örgüyü kullanan şematik Brillouin bölge ve kullanılan brillioun yol Γ -M-K- Γ kırmızı oklar ile gösterilmektedir. H-BP'in atomik konfigürasyonunda kahve ve gri küreler sırasıyla fosfor ve Bor atomlarını temsil etmektedir)

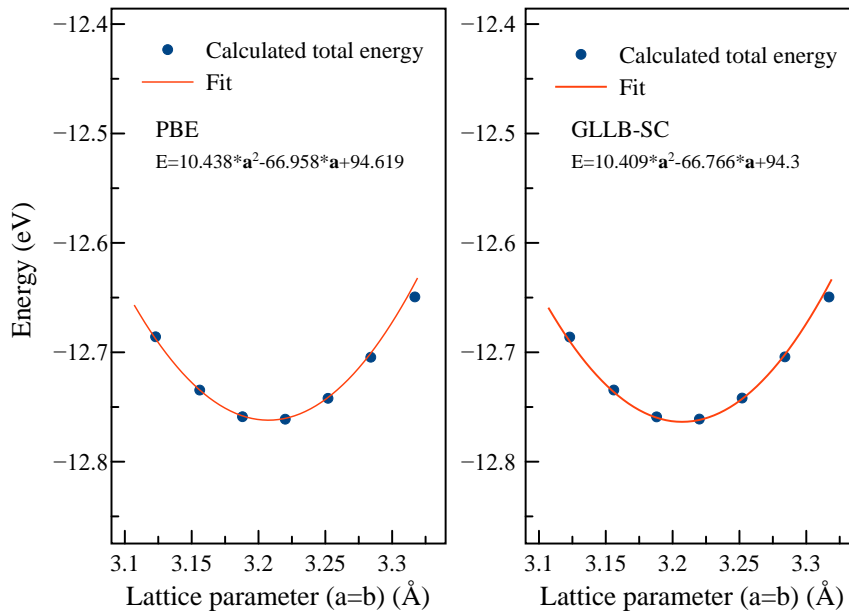


Figure 2. After lattice parameter optimizations, change of lattice parameter depends on total energy for PBE and GLLB-SC as XC's. Energy dependent lattice parameters have been found the optimized lattice parameters using fit plot both PBE and GLLB-SC functionalims (Örgü parametre optimizasyonundan sonra, PBE ve GLLB-SC deęiş tokuş korelasyonları için toplam enerjiye baęlı olarak örgü parametresinin deęişimi)

3. RESULTS (BULGULAR)

Figure 3 shows the electronic band structure and DOS result for unstrained the h-BP monolayer. The energy band gap values for PBE and GLLB-SC are calculated as 0.89 eV and 1.05 eV with a direct band gap at K point, respectively. In literature, the energy band gap of the h-BP monolayer for PBE is consistent with other studies [27]. The calculated energy band gap for GLLB-SC is slightly lower than

HSE06 and GW results [28-30]. However, it gives a more accurate value than standard PBE calculations. It can be said that a more accurate energy band gap as a result of GLLB-SC is obtained with low computing cost according to PBE.

Moreover, the contribution of the orbitals of Boron (B) and Phosphorus (P) is calculated by PDOS calculations and shown in figure 4. The valence band (VB) of h-BP is mostly formed by the p

orbitals of B and P atoms. The p orbital of P atoms has much more contribution than the B atom. However, the more contribution to the conduction band (CB) came from the p orbitals of the B atom. Also, the s orbitals of both atoms have a low density for the VB and CB. For calculated bond lengths (d_B .

ρ) between B and P atoms is given 1.8540 Å for PBE and 1.8516 Å for GLLB-SC, respectively. The bond lengths of h-BP are coherent with found values in the literature [28, 29].

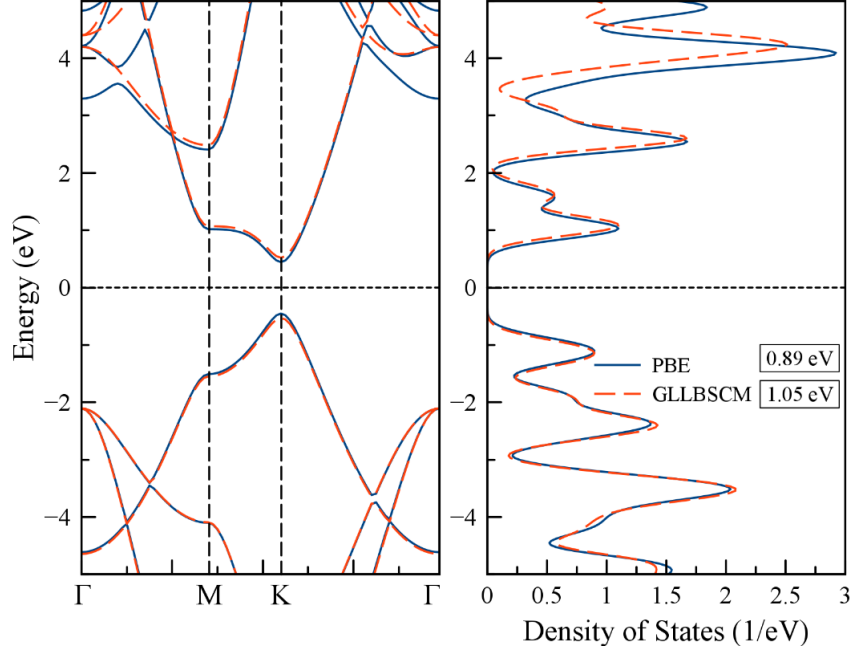


Figure 3. Electronic band structure and DOS of the h-BP monolayer using GLLB-SC and PBE as XCs (Değiş-tokuş korelasyonu olarak GLLB-SC ve PBE kullanılarak h-BP tek tabakanın elektronik band yapısı ve durum yoğunluğu)

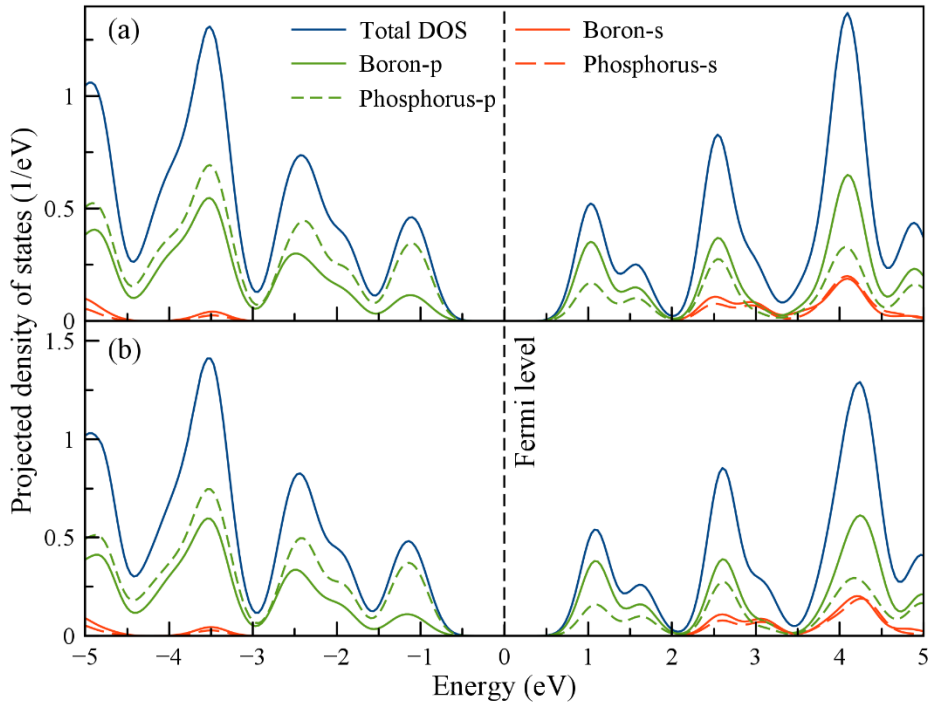


Figure 4. PDOS of the h-BP for a) PBE and b) GLLB-SC (a) PBE ve b) GLLB-SC için h-BP'nin PDOS sonuçları)

After the strain is applied to the h-BP monolayer, the bond length of h-BP for PBE and GLLB-SC are calculated to fit equations are given as $d_{B-P}^{PBE} =$

$1.8523 + 0.0185x$ for PBE and $d_{B-P}^{GLLB-SC} = 1.8515 + 0.0185x$ for GLLB-SC also in here x represents strain. From the fit equations for both

XC's, as the strain is applied on the structure from compressive to tensile step by step, the bond lengths of h-BP are changed almost linearly. As strain is changed from -5% to 5%, the energy band gap values for PBE are changed from 0.667 eV to 1.005 eV in figure 5a. As for energy band gap values of GLLB-SC, the energy band gaps are found at 0.784 eV and 1.241 eV for -5% and 5% in figure 5b. Also, a fit is applied to the energy band gap result of PBE and GLLB-SC. The fit equations are found to be $E_g^{PBE} = 0.8821 + 0.0337x - 0.0019x^2$ for PBE and $E_g^{GLLB-SC} = 1.0539 + 0.0456x - 0.0017x^2$ for GLLB-SC. All calculated energy band gaps show a blue shift for compressive strain and a red shift for tensile strain. The energy band gap changing (ΔE) for PBE and GLLB-SC is found to be 0.338 eV and 0.457 eV, respectively. It is shown that GLLB-SC to adjust the energy band gap with a larger range is given as better results. In literature, a study done by HSE06 is shown 0.456 eV for ΔE value the with same strain range in our study [30]. It is important that although obtained energy band

gaps by GLLB-SC are slightly lower than HSE06, the capability of the tuning energy band gap for these XC's is almost the same. The strain-dependent electronic band structure for both PBE and GLLB-SC show a direct transition-energy band gap at K for the strained and unstrained structure of h-BP.

Strain could affect the energetical stability of the h-BP monolayer, and the total energy values per atom calculated by PBE and GLLB-SC are by table 1. The unstrained h-BP monolayers show more stability for PBE and GLLB-SC. Applying strain to the h-BP monolayer lattice, h-BP has become an energetically unstable structure.

A comparison of both this study and other studies in the literature on energy band gap changing is shown in figure 6. The applied strain values to the h-BP are between $\pm 5\%$. Our results for PBE are very consistent with other results in the literature [24, 33, 34].

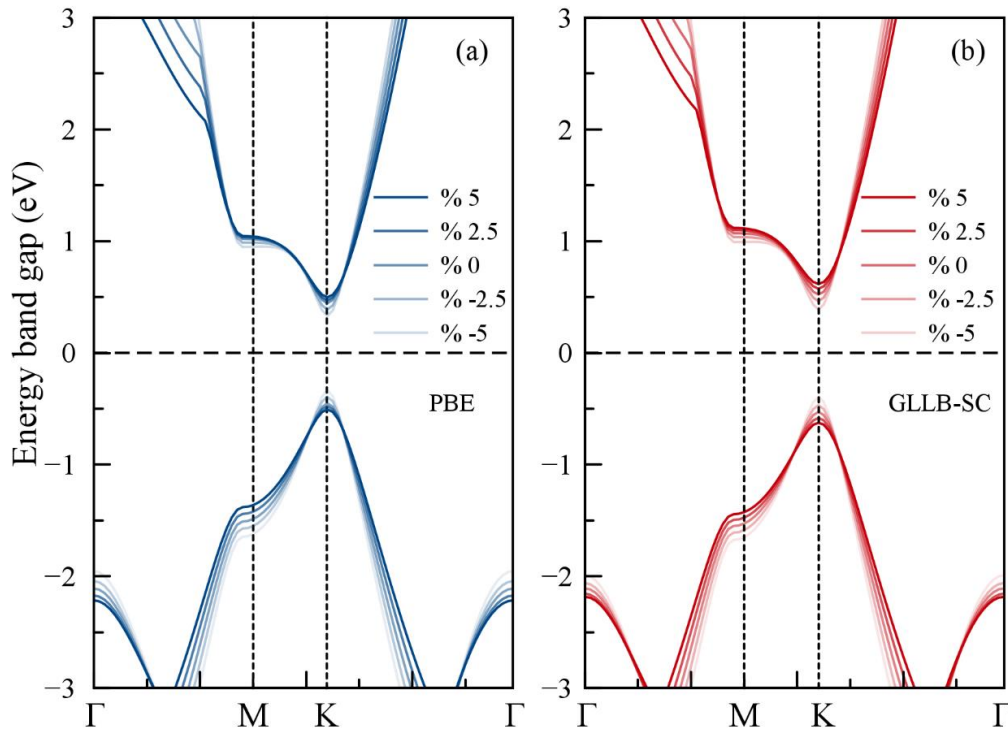


Figure 5. CBM and VBM change depending on strain in the h-BP monolayer using a) PBE and b) GLLB-SC. The applied strain to h-BP is between -5% and 5% for PBE and GLLB-SC functionalims (h-BP tek tabakasında gerginliğe bağlı olarak CBM ve VBM değişimi a) PBE ve b) GLLB-SC. H-BP tek tabakasına uygulanan gerginlik PBE ve GLLB-SC fonksiyonelizmler için -5% ve 5% arasındadır)

Table 1. Summarized the structural and the electronic calculations, the effect of strain on the bond lengths and total energies of the h-BP monolayer. The results are shown both PBE and GLLB-SC functionalism. Both functionalism show that the structural stability according to total energies is decreased under strain (yapısal ve elektronik hesaplamaların özeti, gerginliğin h-BP tek tabakanın bağ uzunluğu ve toplam enerjisine etkisi. Hem PBE hem de GLLB-SC sonuçları görülmektedir. Her iki fonksiyon gerginlik altında toplam enerjiye göre stabilite azalmaktadır.)

Strain (%)	d_{P-B} (Å) with PBE	d_{P-B} (Å) with GLLB-SC	Total energy (eV) per atom with PBE	Total energy (eV) per atom with GLLB-SC
-5	1.7592	1.7589	-5.9581	-6.2654
-2.5	1.8056	1.8052	-6.0343	-6.3491
0	1.8540	1.8515	-6.0591	-6.3785
2.5	1.8981	1.8978	-6.0128	-6.3416
5	1.9444	1.9441	-5.8876	-6.2230

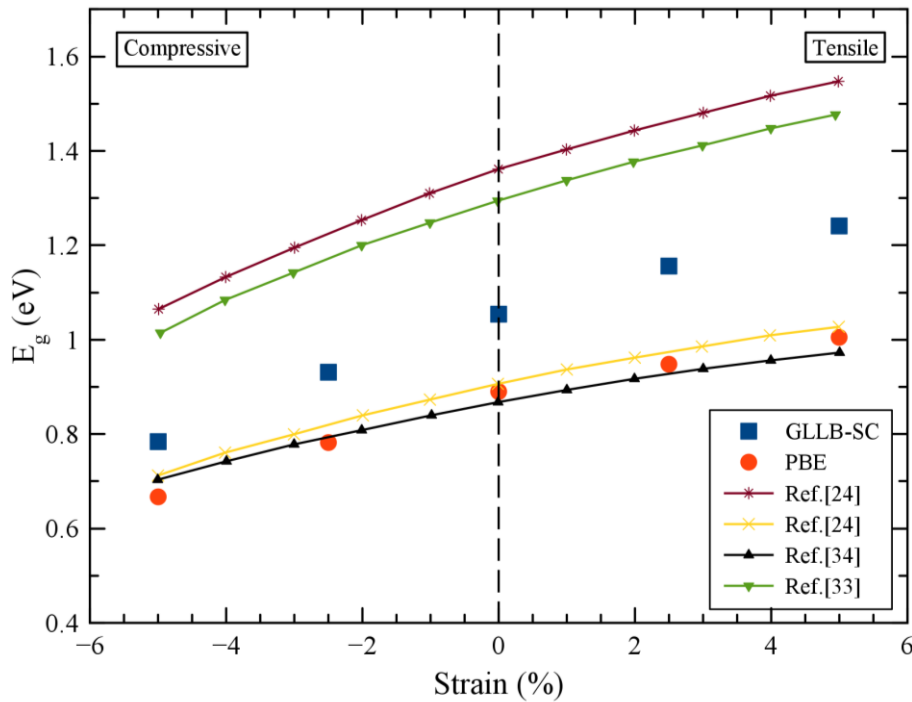


Figure 6. Change in energy band gap dependent on applied strain to h-BP and comparison other studies found in the literature (Literatürde bulunan diğer çalışmaların kıyaslaması ve gerginlik uygulanmış h-BP tek tabakanın yasak bant aralığındaki değişim)

In literature, energy band gaps of h-BP depending on $\pm 5\%$ of the strain are changed from ~ 0.7 to ~ 1 eV for PBE functionalism. As for GLLB-SC calculations, it is lower than a little bit HSE06 results of other studies [24]. Furthermore, energy

band gaps of h-BP in same strain values for HSE06 given similar data to experimental results are found between ~ 1 and ~ 1.5 eV. Due to the lack of the experimental band gap for the h-BP monolayer, the exact band gap of the h-BP cannot be determined up

to now. However, according to our best knowledge, for many 2D materials, the calculated energy band gap results with GLLB-SC include comparable with HSE06 and GW results found in the literature [17, 35]. Also, the investigated strain range of the h-BP, and the increasing trend in the energy band gap for PBE and GLLB-SC in this work are very similar to each.

4. CONCLUSIONS (SONUÇLAR)

The electronic structure of pristine monolayer h-BP is investigated by DFT using the GPAW code implemented in PBE and GLLB-SC as exchange-correlation functionals. For the input parameter interpretation, and result data management, gpaw-tools software is used. The energy band gaps of the monolayer are 0.89 eV and 1.05 eV for PBE and GLLB-SC, respectively. The GLLB-SC which has a low computational cost to HSE06 and GW shows a more accurate electronic structure than PBE for monolayer h-BP. To see the electronic structure behavior of the h-BP against applied strain, electronic band structures are calculated for both tensile and compressive strain regions. As the strain values apply to lattice from -5% to 5%, the calculated energy band gaps have gradually increased. The strained electronic band structures are found to be direct semiconductor properties between the investigated strain values. The obtained strain-dependent electronic and structural properties may be important for the possibility in flexible technology of h-BP monolayers.

ACKNOWLEDGMENTS (TEŞEKKÜR)

I would like to thank Prof. Dr. S. B. Lisesivdin and Prof. Dr. B. Sarikavak-Lisesivdin from the Physics department at Gazi University for the continuous development of *gpaw-tools* script.

DECLARATION OF ETHICAL STANDARDS (ETİK STANDARTLARIN BEYANI)

The author of this article declares that the materials and methods they use in their work do not require ethical committee approval and/or legal-specific permission.

Bu makalenin yazarı çalışmalarında kullandıkları materyal ve yöntemlerin etik kurul izni ve/veya yasal-özel bir izin gerektirmediğini beyan ederler.

AUTHORS' CONTRIBUTIONS (YAZARLARIN KATKILARI)

Polat NARİN: He carried out the numerical calculations, analyzed the results and performed the writing process.

Nümerik hesaplamaları gerçekleştirdi, sonuçlarını analiz etti ve makalenin yazım işlemini gerçekleştirmiştir.

CONFLICT OF INTEREST (ÇIKAR ÇATIŞMASI)

There is no conflict of interest in this study.

Bu çalışmada herhangi bir çıkar çatışması yoktur.

REFERENCES (KAYNAKLAR)

- [1] Fiori, G., Bonaccorso, F., Iannaccone, G., Palacios, T., Neumaier, D., Seabaugh, A., Banerjee, S. K., Colombo, L. (2014). Electronics based on two-dimensional materials. *Nature nanotechnology*, 9(10), 768-779.
- [2] Xu, B., Qi, S., Jin, M., Cai, X., Lai, L., Sun, Z., Han, X., Lin, Z., Shao, H., Peng, P., Xiang, Z., Elshof, J. E., Tan, R., Liu, C., Zhang, Z., Duan, X. & Ma, J. (2019). 2020 roadmap on two-dimensional materials for energy storage and conversion. *Chinese Chemical Letters*, 30(12), 2053-2064.
- [3] Cheng, L., Lee, J., Zhu, H., Ravichandran, A. V., Wang, Q., Lucero, A. T., Kim, M. J., Wallace, R. M. Colombo, L. & Kim, J. (2017). Sub-10 nm tunable hybrid dielectric engineering on MoS₂ for two-dimensional material-based devices. *ACS nano*, 11(10), 10243-10252.
- [4] Dai, M., Wang, Z., Wang, F., Qiu, Y., Zhang, J., Xu, C. Y., Zhai, T., Cao, W., Fu, Y., Jia, D., Zhou, Y., & Hu, P. A. (2019). Two-dimensional van der Waals materials with aligned in-plane polarization and large piezoelectric effect for self-powered piezoelectric sensors. *Nano letters*, 19(8), 5410-5416.
- [5] Oughaddou, H., Enriquez, H., Tchalala, M. R., Yildirim, H., Mayne, A. J., Bendounan, A., Dujardin, G., Ali, M. A., Kara, A. (2015). Silicene, a promising new 2D material. *Progress in Surface Science*, 90(1), 46-83.
- [6] Li, L., Lu, S. Z., Pan, J., Qin, Z., Wang, Y. Q., Wang, Y., Cao, G. Y., Du, S., Gao, H. J. (2014). Buckled germanene formation on Pt (111). *Advanced Materials*, 26(28), 4820-4824.
- [7] Akhtar, M., Anderson, G., Zhao, R., Alruqi, A., Mroczkowska, J. E., Sumanasekera, G., Jasinski, J. B. (2017). Recent advances in synthesis, properties, and applications of phosphorene. *npj 2D Materials and Applications*, 1(1), 1-13.
- [8] Manzeli, S., Ovchinnikov, D., Pasquier, D., Yazyev, O. V., Kis, A. (2017). 2D transition metal dichalcogenides. *Nature Reviews Materials*, 2(8), 1-15.

- [9] Zhang, K., Feng, Y., Wang, F., Yang, Z., Wang, J. (2017). Two dimensional hexagonal boron nitride (2D-hBN): synthesis, properties and applications. *Journal of Materials Chemistry C*, 5(46), 11992-12022.
- [10] Wang, S. F., Wu, X. J. (2015). First-principles study on electronic and optical properties of graphene-like boron phosphide sheets. *Chinese Journal of Chemical Physics*, 28(5), 588.
- [11] Varley, J. B., Miglio, A., Ha, V. A., van Setten, M. J., Rignanese, G. M., Hautier, G. (2017). High-throughput design of non-oxide p-type transparent conducting materials: data mining, search strategy, and identification of boron phosphide. *Chemistry of Materials*, 29(6), 2568-2573.
- [12] Xie, M., Zhang, S., Cai, B., Zhu, Z., Zou, Y., Zeng, H. (2016). Two-dimensional BX (X= P, As, Sb) semiconductors with mobilities approaching graphene. *Nanoscale*, 8(27), 13407-13413.
- [13] Chen, Y., Zhang, X., Qin, J., & Liu, R. (2021). High-throughput screening of single metal atom anchored on N-doped boron phosphide for N₂ reduction. *Nanoscale*, 13(31), 13437-13450.
- [14] Obeid, M. M., Jappor, H. R., Al-Marzoki, K., Hoat, D. M., Vu, T. V., Edrees, S. J., Yaseen, Z. M., Shukur, M. M. (2019). Electronic and magnetic properties of single-layer boron phosphide associated with materials processing defects. *Computational Materials Science*, 170, 109201.
- [15] Galicia-Hernandez, J. M., Guerrero-Sanchez, J., Ponce-Perez, R., Fernandez-Escamilla, H. N., Cocoltzi, G. H., & Takeuchi, N. (2022). Self-energy corrected band-gap tuning induced by strain in the hexagonal boron phosphide monolayer. *Computational Materials Science*, 203, 111144.
- [16] Yazdanmehr, M., Asadabadi, S. J., Nourmohammadi, A., Ghasemzadeh, M., Rezvanian, M. (2012). Electronic structure and bandgap of γ -Al₂O₃ compound using mBJ exchange potential. *Nanoscale research letters*, 7(1), 1-10.
- [17] Tran, F., Blaha, P. (2017). Importance of the kinetic energy density for band gap calculations in solids with density functional theory. *The Journal of Physical Chemistry A*, 121(17), 3318-3325.
- [18] Tran, F., Doumont, J., Kalantari, L., Blaha, P., Rauch, T., Borlido, P., Botti, S., Marques, M. A. L. Patra, A., Jana, S., Samal, P. (2021). Bandgap of two-dimensional materials: Thorough assessment of modern exchange–correlation functionals. *The Journal of Chemical Physics*, 155(10), 104103.
- [19] Gritsenko, O., van Leeuwen, R., van Lenthe, E., Baerends, E. J. (1995). Self-consistent approximation to the Kohn-Sham exchange potential. *Physical Review A*, 51(3), 1944.
- [20] Castelli, I. E., Hüser, F., Pandey, M., Li, H., Thygesen, K. S., Seger, B., Jain, A., Persson, K. A. Ceder, G., Jacobsen, K. W. (2015). New light-harvesting materials using accurate and efficient bandgap calculations. *Advanced Energy Materials*, 5(2), 1400915.
- [21] Ullah, S., Denis, P. A., Menezes, M. G., Sato, F. (2019). Tunable optoelectronic properties in h-BP/h-BAs bilayers: the effect of an external electrical field. *Applied Surface Science*, 493, 308-319.
- [22] Luo, Z., Ma, Y., Yang, X., Lv, B., Gao, Z., Ding, Z., Liu, X. (2020). Native Point Defects in Monolayer Hexagonal Boron Phosphide from First Principles. *Journal of Electronic Materials*, 49(10), 5782-5789.
- [23] Naumis, G. G., Barraza-Lopez, S., Oliva-Leyva, M., Terrones, H. (2017). Electronic and optical properties of strained graphene and other strained 2D materials: a review. *Reports on Progress in Physics*, 80(9), 096501.
- [24] Li, F. Q., Zhang, Y., Zhang, S. L. (2021). Defects and Strain Engineering of Structural, Elastic, and Electronic Properties of Boron-Phosphide Monolayer: A Hybrid Density Functional Theory Study. *Nanomaterials*, 11(6), 1395.
- [25] Enkovaara, J., Rostgaard, C., Mortensen, J. J., Chen, J., Duřak, M., Ferrighi, L., Gavnholt, J., Glinsvad, Haikola, V., Hansen, H. A. Kristoffersen, H. H., Kuisma, M., Larsen, A. H., Lehtovaara, L., Ljungberg, M., Lopez-Acevedo, O., Moses, P. G., Ojanen, J., Olsen, T., Petzold, V., Romero, N. A., Stausholm-Møller, J., Strange, M., Tritsaris, G. A., Vanin, M., Walter, M., Hammer, Häkkinen, V. H., Madsen, G. K. H., Nieminen, R. M., Nørskov, J. K., Puska, M., Rantala, T. T., Schiøtz, J., Thygesen, K. S., Jacobsen, K. W. (2010). Electronic structure calculations with GPAW: a real-space implementation of the projector augmented-wave method. *Journal of physics: Condensed matter*, 22(25), 253202.
- [26] Lisesivdin, S. B., Sarikavak-Lisesivdin, B. (2022). gpaw-tools–higher-level user interaction scripts for GPAW calculations and interatomic potential based structure optimization. *Computational Materials Science*, 204, 111201.
- [27] Şahin, H., Cahangirov, S., Topsakal, M., Bekaroglu, E., Akturk, E., Senger, R. T., Ciraci, S. (2009). Monolayer honeycomb structures of

- group-IV elements and III-V binary compounds: First-principles calculations. *Physical Review B*, 80(15), 155453.
- [28] Zeng, B., Li, M., Zhang, X., Yi, Y., Fu, L., Long, M. (2016). First-principles prediction of the electronic structure and carrier mobility in hexagonal boron phosphide sheet and nanoribbons. *The Journal of Physical Chemistry C*, 120(43), 25037-25042.
- [29] Hasan Khan, M. S., Islam, M. R., Hasan, M. T. (2020). Strain-dependent electronic and optical properties of boron-phosphide and germanium-carbide hetero-bilayer: A first-principles study. *AIP Advances*, 10(8), 085128.
- [30] Çakır, D., Kecik, D., Sahin, H., Durgun, E., Peeters, F. M. (2015). Realization of ap-n junction in a single layer boron-phosphide. *Physical Chemistry Chemical Physics*, 17(19), 13013-13020.
- [31] Islam, M. R., Liu, K., Wang, Z., Qu, S., Zhao, C., Wang, X., Wang, Z. (2021). Impact of defect and doping on the structural and electronic properties of monolayer boron phosphide. *Chemical Physics*, 542, 111054.
- [32] Cheng, Y., Meng, R., Tan, C., Chen, X., Xiao, J. (2018). Selective gas adsorption and I-V response of monolayer boron phosphide introduced by dopants: A first-principle study. *Applied Surface Science*, 427, 176-188.
- [33] Wang, Y., Huang, C., Li, D., Huang, F., Zhang, X., Huang, K., Xu, J. (2019). Stress-and electric-field-induced band gap tuning in hexagonal boron phosphide layers. *Journal of Physics: Condensed Matter*, 31(46), 465502.
- [34] Yu, J., Guo, W. (2015). Strain tunable electronic and magnetic properties of pristine and semihydrogenated hexagonal boron phosphide. *Applied Physics Letters*, 106(4), 043107.
- [35] Tran, F., Ehsan, S., Blaha, P. (2018). Assessment of the GLLB-SC potential for solid-state properties and attempts for improvement. *Physical Review Materials*, 2(2), 023802.